INTERNATIONAL JOURNAL OF HYDROGEN ENERGY 42 (2017) 18014–18027

Available online at www.sciencedirect.com

ScienceDirect

journal homepage: www.elsevier.com/locate/he

Investigation of dynamic heat transfer process through coaxial heat exchangers in the ground

*Mohamed Salah Saadi, Rabah Gomri**

Université Frères Mentouri Constantine 1, Department of Génie Climatique, 25000, Constantine, Algeria

ARTICLE INFO

Article history:
Received 14 November 2016
Received in revised form
2 March 2017
Accepted 17 March 2017
Available online 12 April 2017

Keywords:
Borehole heat exchanger
Finite volume method (FVM)
Finite Line Source (FLS)
Transient heat problem
Thermal interferences
Ground Source Heat Pump (GSHP)

ABSTRACT

Recently, researchers are focussing on using ground coupled heat pump systems as a heat source or sink rather than air source heat pumps for HVAC needs due to the stable temperature and the high thermal inertia of the soil. The investment cost of these systems is too expensive therefore the precise thermal analysis, design and parameter optimization are essential. For an accurate design, the maximum of physical phenomena such as: axial effects, seasonal effects, underground water flow and BHE dynamic behaviour must be accounted for in order to reflect exactly the real physical situation. In the present paper thermal interferences are investigated under seasonal effects and a dynamic heat flux for a vertical coaxial borehole heat exchangers field. This enables to avoid thermal interferences by predicting efficient period of operation corresponding to the beginning of the studied phenomena (interferences) for a given separation distance between two boreholes. To reach this purpose, as a first step, a transient 2D Finite volume method (FVM) for a single borehole heat exchanger was built using MATLAB, which accounts for accurate axial and seasonal effects and a dynamic heat flux that is function of depth and time. This model has been validated against the Finite Line Source (FLS) analytical solution and good agreement between analytical and numerical methods has been obtained. Then the model has been extended to a quasi-3D model in order to investigate thermal interferences between two neighbouring boreholes. After 500 h and at the mid-point of the separating distance (1.5 m) where interferences are the strongest, the temperature is 50% (6.64 °C) lower than the case where there are no interferences.

Introduction

Our society has become dependent on fossil fuels such as oil, coal and natural gas. Over-usage of these sources for energy results in emissions of greenhouse gases including carbon dioxide (CO_2). These gases cause undesirable changes in the climate. Geothermal energy is energy derived from the heat of the earth. It is a clean resource, renewable and sustainable. Resources of geothermal energy range from the shallow ground to hot water and hot rock found a few miles beneath the Earth's surface, and down even deeper to the extremely high temperatures of molten rock called magma. Many technologies have been developed to take advantage of geothermal energy: Generating electricity from the earth's heat [1], producing heat directly from hot water within the earth [1], geothermal hydrogen production [1,2], using the shallow ground to heat and cool buildings [3–5].

* *Corresponding author.*
E-mail address: rabahgomri@yahoo.fr (R. Gomri).
http://dx.doi.org/10.1016/j.ijhydene.2017.03.106

Nomenclature

a	Temperature coefficient
alb	Soil albedo
A	Amplitude of the temperature wave
b_1, b_2	Constants
c	Volumetric heat capacity (J/K m^3)
C_1, C_2, C_3, C_4	Constants
CE	Convective energy (W/m^2)
G	Solar radiation (w/m^2)
h	Integral parameter
HTC	Heat transfer coefficient (W/m^2 K)
k	Conductivity (W/K m)
L	Well depth (m)
LE	Long wave radiation emitted from the ground surface (W/m^2)
LR	Absorbed solar radiations (W/m^2)
P	Period (hour)
q	Heating rate for line source (W/m)
r	Radial coordinate (m)
R	Thermal resistance (K m/W)
T	Temperature (°C)
t_0	The time lag needed for the soil surface temperature to reach T_m
T_m	Annual mean temperature (°C)
u	Wind velocity (m/s)
V	Control volume
w	Volumetric fluid flow rate (m^3/s)
z	Axial coordinate (m)

Greek symbols

α	Thermal diffusivity (m^2/s)
γ	Inverse of damping depth (cm^{-1})
δ_i	Constants
σ	Stephan Boltzmann constant 5.67 10^{-8} (W/m^2 K)
φ	Relative humidity of the air

Subscripts

0	Initial values
1	Flow path number one
2	Flow path number two
b	Borehole
D	Dimensionless
e	Eastern node
fi	Circulating fluid inside of inner pipe
fo	Circulating fluid outside of inner pipe
in	Inlet
m	Mean value
n	Northern node
P	The centre of the node
pw	Pipe wall
rs	Reference value for ground
s	Southern node
S	Soil
Surf	Surface
w	Western node
wat	Water
z	Depth

Abbreviations

BHE	Borehole heat exchanger
FLS	Finite line source
FVM	Finite volume method

Below a certain depth, the ground generally remains thermally stable. This attracted researchers' attention to exploit the thermal stability of the ground; the ground could be used as a heat sink in summer by storing a heat amount which was extracted from an air conditioned space during summer season, and as a heat source in winter for air conditioning too using the inverse process, this is could be concretized using a heat pump device [3]. Ground Source Heat Pump (GSHP) is a modern technology used for heating and cooling of buildings. GSHP consists of ground itself to store or extract heat, heat pump to convert that heat to a suitable temperature level, and the equipment inside the building transferring the heat into or from the rooms. Many technologies of GSHP have been realized in several configurations, according to the heat exchanger position, horizontal or vertical. Due to the fact that the deep ground is more thermally stable it is opted for the vertical ones (Fig. 1).

The heat transfer process inside and outside the borehole heat exchanger (BHE) has an impact on the storage efficiencies and the borehole parameters prediction which means the borehole design and parameters prediction like the appropriate depth, diameter, thermal response test (TRT) which yield the borehole thermal resistance and the ground conductivity, which makes it important to perform an accurate heat transfer analysis.

Due to the fact of the high first investment cost of the BHEs, it is recommended to design them as accurate as possible, and simulation of fluid and surrounding ground temperatures distributions represents a good tool to achieve an accurate design and gives a better understanding of the heat transfer process. For this reason, several models have been developed which are analytical [6–18] and numerical [19–32] methods.

For analytical method, Zeng et al. [6] studied a 2D unsteady state analytical solution and a semi analytical solution. Lamarche and Beauchamp [7] starting from Zeng's work, they gave the analytical solution of the expression of the borehole wall integral mean temperature by integrating along the borehole depth. Bandos et al. [8] derived a solution to the three-dimensional finite line source model for borehole heat exchangers that takes into account the prevailing geothermal gradient and allows arbitrary ground surface temperature changes. They derived analytical expressions for the average ground temperature. In addition, a self-consistent procedure to evaluate the in situ thermal response test (TRT) data is

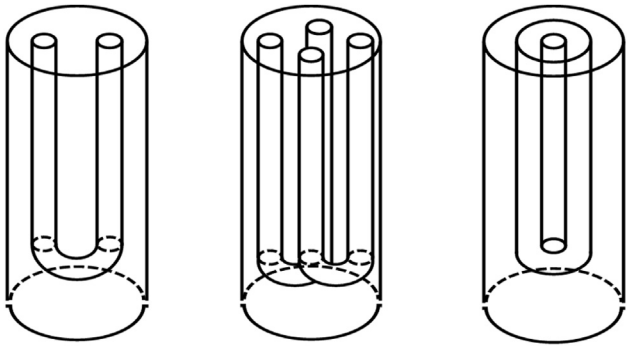

Fig. 1 – The three common used borehole configurations.

outlined, knowing that the purpose of TRT is to define the BHE thermal resistance and the soil thermal conductivity. Comparing the results obtained using the finite and infinite line source methods, Marcotte et al. [9] concluded that the borehole length is 15% shorter when axial conduction effects are considered, also dealing with underground water freezing, the amount of energy that has to be removed to freeze the ground is three times higher when axial effects are considered as the mean value of the temperature distribution. Molina-Giraldo et al. [10] developed a new analytical approach which considers both effects: groundwater flow and axial effects. They concluded that axial effects problem is even more important for long simulation times and short borehole lengths. Kurevija et al. [11] used ASHRAE/Kavanaugh in order to investigate the effect of the imbalance amounts of the injected and withdrawn energy from/to the ground as well as thermal interferences on the ground and working fluid temperature changes for a U tube configuration. Hecht-Méndez et al. [12] presented a combined simulation–optimization procedure to simulate the heat transfer in a multiple borehole heat exchangers field when groundwater flow exists and for a mean borehole temperature using temporally and spatially superimposed moving line source equations. They found that borehole output temperature can be raised when optimal extraction rates are used. Li and Lai [13] developed a new line source model which fitted experimental data and TRT better than the common line source model in an isotropic field, the main idea was to build a composite-medium line source model. The obtained results are validated by a reported laboratory experiment. They conclude that model can reproduce experimental temperature responses at short times. Wagner et al. [14] expanded the field of application of the commonly used thermal response test (TRT) to determine the heat transfer parameters of the subsurface. The analytical approach expands the field of application of the TRT to advection-influenced conditions beyond a Darcy velocity of 0.1 m day^{-1}. Cimmino et al. [15] examined the thermal response of U-tube borefield by applying the principle of temporal superposition in the analytical finite line source method in order to account for varying heat fluxes but for an average wall temperature and heat flux rate. Li et al. [16] studied the effect of the short circuiting on the TRT results, and they concluded that the lager short-circuiting loss rate would lead to a greater error for effective subsurface conductivity estimation. Zhang et al. [17] gave an improved optimization method for thermal performance of BHE that was based on analytical solution model, which studies the impacts of inlet fluid temperature, fluid flow rate and borehole depth. Choi and Ooka [18] experimentally examined the effect of natural convection on TRTs for two different grouted boreholes, cement-grouted and gravel-backfilled at two different heat injection rates (approximately 45 W/m and 90 W/m).

For numerical modelling, Yavuzturk et al [19] examined the transient short time response inside and outside the borehole using the 2D finite volume method, their model is capable of predicting the pipe surface temperature with an average relative error of 61% for the first hours of simulation compared to the analytically calculated temperature and became insignificant before the end of 192 h. To get more accurate results, Asinari [20] has built a finite-volume and finite-element hybrid technique, using an explicit scheme and a new grid generation which is compatible for this hybrid method, but the technique increases the computational time. In order to compromise between having accurate results with the shortest time calculation, Kim et al. [21] used a finite element method where they reduced the nodes order as they used a variable time step, and the computational time have been reduced by 95%. Wołoszyn and Goła [22] presented a one-dimensional finite element numerical model for a single vertical borehole heat exchanger working with underground heat storage, which describes the process of heat exchange and divides the grout region into 3 subzones in order to better predict the fluid temperature. Yoon et al. [23] performed a numerical and experimental study on the evaluation of borehole thermal resistance of a vertical closed-loop where the good prediction by using a multipole method, also that the ground thermal conductivity was slightly greater when using the W shape pipe configuration instead of U shape. In order to investigate the thermal interaction of these systems, Koohi-Fayegh and Rosen [24] focused on the two-dimensional transient conduction of heat in the soil around vertical ground U-tube heat exchangers using the numerical code FLUENT, where they considered a constant heat flow rate along the borehole length. Pasquier and Marcotte [25] focused on having a reasonable solution time, a quasi-3D model was developed using spectral methods and it is used as a response model. They showed that the combined use of a spectral method and response model provides, in a few seconds, a temperature solution whose error is below or comparable to the measurement's uncertainty. Luo et al. [26] presented the results from experimental study of borehole heat exchangers three similar fields of different pipe diameters, it has been observed for the first years the larger is the diameter the higher is the efficiency but after a longer period it has been reversed because of highly thermal interference between greater diameter pipes. BniLam and Al-Khoury [27] developed a spectral model to illustrate the effect of friction on heat transfer in the borehole. The studied effect of friction is illustrated in a heat generation due to the caused resistance between the fluid and the pipe internal wall. The analysis shows that, for the geometry and materials typically utilized in shallow geothermal systems, the friction at pipe wall is not really significant. However, the main advantage is on the solution technique that can be useful for fluid flow in narrow

pipes, high fluid velocities, high fluid viscosities, and complex geometry. The method can be useful for solving other non-homogeneous coupled partial differential equations. Hein et al. [28] presented a numerical study to observe the evolution of BHE outflow and soil temperature. It has been observed that outflow and soil temperature will gradually drop until they reach a quasi-steady-state. It was also found that groundwater flow and using BHE for cooling will be beneficial to the energy recovery. Hein et al. [29] presented a numerical model in order to evaluate the available amount of shallow geothermal energy by using borehole heat exchanger coupled to ground Source heat pump systems. Numerical analyses have been performed by simulating the long-term evolution of the subsurface temperature field, which is subject to the operation of borehole heat exchangers and varying parameters like subsurface thermal conductivity and groundwater flow velocity. Baek et al. [30] developed a three-dimensional equivalent transient ground heat exchanger. They investigated the effects of amount of geothermal load, duration of the recovery time per day, and daily geothermal load pattern on the ground temperature recovery. The effects of the geothermal load on ground temperature recovery were also analysed under different soil thermal conductivity conditions. These results demonstrate the importance of considering the recovery time in the ground heat exchanger design stage to reduce the borehole length. Gallero et al. [31] presented a model based on the use of the electrical analogy to model heat transfer within the borehole and thermal response factors (short and long time-step g-functions) to estimate heat flow to the surrounding of a single U-tube ground heat exchanger. The model has been validated experimentally by using the reference data sets drawn from two tests (constant heat input rate and interrupted tests) made under controlled laboratory conditions. The results have also been compared with the simulated. Florides et al. [32] presented a mathematical model of vertical and horizontal ground heat exchangers (GHEs) and compares their efficiency. The model used calculates the heat flow in the fluid, tubes, grout and ground. The vertical U-tube GHE is represented by two 100 m lines, embedded in four different types of ground with an additional bottom base. The horizontal GHE consists of four 50 m tube lines embedded in three ground layers. Comparisons between horizontal and vertical GHEs revealed that under the same operating conditions and centre-to-centre distances of the tubes, the vertical GHE keeps a much lower mean temperature. Simulations for a horizontal GHE, for a 50 h of continuous operation period and 24 °C initial ground temperature, showed that the mean fluid temperature can remain lower than that of the vertical GHE if the centre-to-centre- distance of the tubes increases to 1 m.

It can be concluded that analytical models are faster and require less calculating power than numerical models, and numerical models have the capability to treat easily a higher number of physical phenomena thus a more exact physical situation. Most of the models focus on thermal response tests (TRTs), thermal analysis, borehole performances, design and optimization.

In the present paper, thermal interferences are investigated under seasonal effects and a dynamic heat flux rate, where seasonal effects are treated as a variable convective flux at the surface (which is function of the radius on the surface). First, a 2D unsteady numerical model has been established which accounts for axial and seasonal effects and a dynamic behaviour of the withdrawn heat flux for a coaxial borehole surroundings. A comparison between two different ways of accounting for seasonal effects is presented: the first considers a variable ground surface temperature oscillations (the undisturbed temperature), the second accounts for a variable exchanged convective heat flux with the atmosphere. For the fluid side, the model has been coupled with an analytical model that provides the fluid temperature distribution for the coaxial configuration, rather than using the mean value of the fluid temperature, thus a dynamic heat flux at the borehole wall is accounted and which is function of time and depth. Then, the model has been extended to a quasi 3D one in order to investigate thermal interferences between two neighbouring boreholes under dynamic heat extraction (fluid temperature distribution function of depth and time), and seasonal effects simultaneously.

Mathematical model

Transient heat conduction in the soil is represented here in two dimensions. Some assumptions are made for the present model:

- Soil and material properties do not vary with temperature. Although thermal properties of soils (thermal conductivity and specific heat capacity) are temperature dependent [33], constant thermal properties can be assumed because the change in temperature is not significant in this study.
- Heat transfer in the soil is a pure conduction. Because the medium is assumed to be dry which implies thermally induced water flow is not expected.

The transient conduction equation in polar coordinates is expressed as follows:

$$\frac{1}{\alpha}\cdot\frac{\delta T}{\delta t}=\frac{1}{r}\cdot\frac{\delta T}{\delta r}\cdot\left(r\cdot\frac{\delta T}{\delta r}\right)+\frac{\delta}{\delta z}\left(\frac{\delta T}{\delta z}\right) \quad (1)$$

The term on the left side represents the transient effects. The first term on the right side is the heat flux components in the radial direction (r) and the second term is related to the axial direction (z).

This equation has been discretized using a fully implicit finite volume approach [34,35]. For numerical analysis, the continuous problem is converted into an algebraic problem by integrating over time and space as follows:

$$\int_t^{t+\Delta t}\int_{CV}\mathrm{div}[\mathrm{grad}(T)]\cdot dV\cdot dt=\int_t^{t+\Delta t}\int_{CV}\frac{1}{\alpha}\frac{\delta T}{\delta t}dV\cdot dt \quad (2)$$

For radial and axial coordinates:

$$dV=dr\cdot dz \quad (3)$$

This leads to:

$$a_P\cdot T_P=a_P^0\cdot T_P^0+a_n\cdot T_n+a_s\cdot T_s+a_e\cdot T_e+a_w\cdot T_w \quad (4)$$

where a_p^0, a_e, a_w, a_n and a_s are the temperatures coefficients given by the following equations:

$$a_p^0 = \frac{(r_w^2 - r_e^2)\cdot\Delta z}{2\cdot\alpha\cdot\Delta t} \quad (5)$$

$$a_e = r_e\cdot\frac{\Delta z}{\Delta r} \quad (6)$$

$$a_w = r_w\cdot\frac{\Delta z}{\Delta r} \quad (7)$$

$$a_n = \frac{(r_w^2 - r_e^2)}{2\cdot\Delta z_n} \quad (8)$$

$$a_s = \frac{(r_w^2 - r_e^2)}{2\cdot\Delta z_s} \quad (9)$$

The resulting algebraic equations are linear and solved reasonably efficiently using the TDMA algorithm [34,35] which uses the back substitution algorithm technique.

Grid generation

This part treats the location of the control volume faces (Fig. 2). There are two possibilities to build this meshing grid, in the first approach faces are placed at the midway between the grid points that provides a good accuracy in calculating the heat flux between the faces but the temperature T_p cannot be regarded as a good representative value of the control volume. In the second approach, the grid points that are placed at the centre of the control volume which enables to better handle the boundary conditions.

Initial and boundary conditions

Accurate boundary conditions lead to differences with previous models for the case of pure heat conduction in the surrounding soil. At the borehole wall side a Neumann boundary condition is considered, which is an imposed heat flux. This flux is modelled by Beier et al. [36] where it is not calculated iteratively when coupled with the ground model which reduces the calculation time, as it provides a depth and time varying heat flux rate. The upper and the lower sides, for the first results, temperature is imposed by coupling to the undisturbed ground temperature model which is function of time and depth. The results are compared to those when these boundaries turn to imposed fluxes, the top side flux become a function not only of time but of the radial direction as well, this is due to the fact that the radial temperature distribution is not a constant value, thus, the amount of heat convection between the soil surface and the ambient air varies at each radius value. This heat flux is modelled by Mihalakakou et al. [37] for an undisturbed soil temperature. For the bottom side, the temperature is substituted by a geothermal heat flux. At the far field radius, which could be predicted by Eskilson [38] ($r = 3\times(\alpha\cdot t)^{0.5}$), the undisturbed ground temperature is imposed and function of time and depth [39]. For the initial values, the undisturbed ground temperature is considered (Fig. 3).

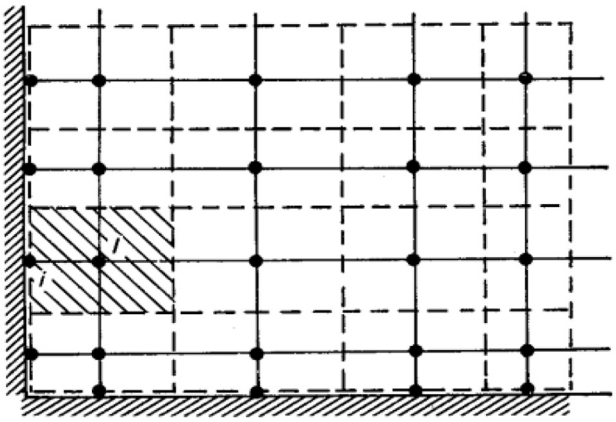

Fig. 2 – Boundary control volumes [33].

Undisturbed ground temperature

This is the ground temperature profile before the system is operating, which is given by Ozgener et al. [39] as follows:

$$T(z,t) = T_m + A_z\sin\left[\frac{2\pi}{P}(t - t_0) - \gamma z - \frac{\pi}{2}\right] \quad (10)$$

where

$$\gamma = \sqrt{\frac{\pi}{\alpha\, P}} \quad (11)$$

The values of T_m, A_Z, t_0 and P are as follow:

$T_m = 17.4788\ ^\circ C$
$A_Z = 42.9\ ^\circ C$
$T_0 = 2850$ h
$P = 8760$ h

Variable heat rate

Most of previous models are based on the assumption of a constant heat flux and if it is not the case they study the dynamic behaviour of the U-tube heat exchanger. In this study, we treat the dynamic behaviour of the coaxial heat exchanger. To do that, temperature profiles along the borehole depth was predicted by the method given in Beier et al. [36].

First of all, the fluid temperatures (downward and upward) were given by a differential form after doing an energy balance.

The downward fluid temperature differential equation:

$$\frac{\partial T_{D1}}{\partial Z_D} = N_{12}\cdot(T_{D2} - T_{D1}) + N_{S1}\cdot(T_{DS} - T_{D1}) \quad (12)$$

The upward fluid temperature differential equation:

$$-\frac{\partial T_{D1}}{\partial Z_D} = N_{12}\cdot(T_{D1} - T_{D2}) + N_{S2}\cdot(T_{DS} - T_{D2}) \quad (13)$$

The solution of Equations (12) and (13) is given by:

The downward fluid dimensionless temperature is expressed as follows:

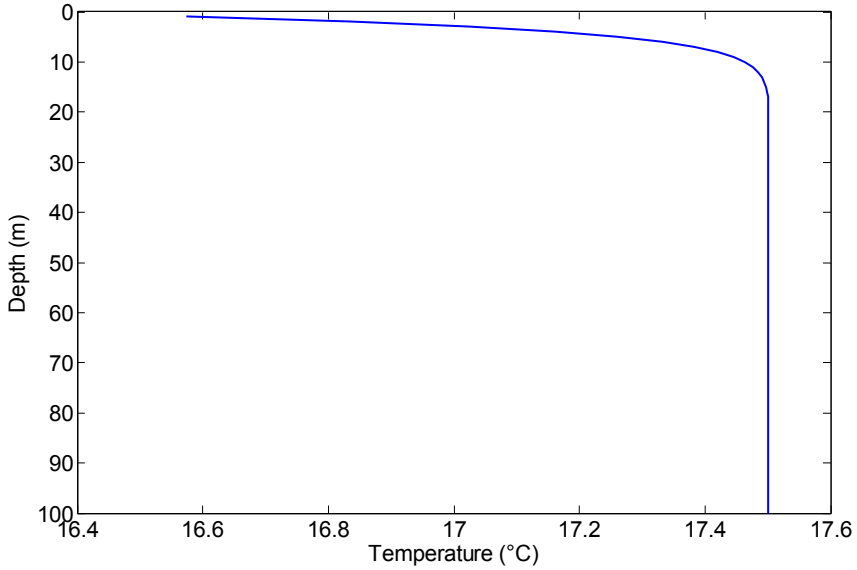

Fig. 3 – Initial soil temperature profile.

$$T_{D_1}(Z_D) = C_1 \cdot e^{b_1 \cdot Z_D} + C_2 \cdot e^{b_2 \cdot Z_D} + I_{11}(Z_D) + I_{12}(Z_D) \quad (14)$$

The upward fluid temperature can be calculated as follows:

$$T_{D_2}(Z_D) = C_3 \cdot e^{b_1 \cdot Z_D} + C_4 \cdot e^{b_2 \cdot Z_D} + I_{21}(Z_D) + I_{22}(Z_D) \quad (15)$$

where

$$Z_D = \frac{z}{L} \quad (16)$$

and

$$T_D = \frac{T(z) - T_{rs}}{T_{in} - T_{rs}} \quad (17)$$

The coefficients C_1, C_2, C_3 and C_4 represent the boundary conditions of the fluid differential equations [36]:

$$C_1 = \frac{(\delta_2 - 1) \cdot e^{b_2} + +I_{11}(1) + I_{12}(1) + I_{21}(1) + I_{22}(1)}{-(\delta_1 - 1) \cdot e^{b_1} + (\delta_2 - 1) \cdot e^{b_2}} \quad (18)$$

$$C_2 = 1 - C_1 \quad (19)$$

$$C_3 = \delta_1 \cdot C_1 \quad (20)$$

$$C_4 = \delta_2 \cdot C_2 \quad (21)$$

where

$$\delta_1 = \frac{N_{S1} + N_{12} + b_1}{N_{12}} \quad (22)$$

$$\delta_2 = \frac{N_{S1} + N_{12} + b_2}{N_{12}} \quad (23)$$

$$b_1 = \frac{-(N_{S_1} - N_{S_2})^2 + 4 \cdot [(N_{12} + N_{S_1}) \cdot (N_{12} + N_{S_2}) - N_{12}^2]^{1/2}}{2} \quad (24)$$

$$b_2 = \frac{-(N_{S_1} - N_{S_2})^2 - 4 \cdot [(N_{12} + N_{S_1}) \cdot (N_{12} + N_{S_2}) - N_{12}^2]^{1/2}}{2} \quad (25)$$

where the parameters N_{12}, N_{S_1} and N_{S_2} represent the dimensionless conductances (the inverse of resistance). The conductance N_{12} corresponds to the heat transfer between the fluids in the inner pipe and the annulus while conductances N_{S_1} and N_{S_2} correspond to the heat exchange between the circulating fluid in the entering pathway and the ground. The formulation of these conductances are given in equations 26–28.

$$N_{S_1} = \frac{L}{w \cdot c_{wat} \cdot (R_{b_1} + R_S)} \quad (26)$$

$$N_{S_2} = \frac{L}{w \cdot c_{wat} \cdot (R_{b_2} + R_{S_1})} \quad (27)$$

$$N_{12} = \frac{L}{w \cdot c_{wat} \cdot R_{12}} \quad (28)$$

where

$$R_{12} = R_{fi} + R_{pw} + R_{fo} \quad (29)$$

R_{b_1} and R_{b_2} are the borehole resistances when the fluid enters the annulus and the inner pipe respectively. More details about I_{11}, I_{12}, I_{21}, I_{22} and the resistances R_{fi}, R_{pw} and R_{fo} can be found in Beier et al. [37].

According to Carslaw and Jaeger [40] the soil resistance is function of time as follows:

$$R_S = \frac{1}{4\pi k_S} \ln\left(\frac{4\alpha t}{\gamma r_b^2}\right) \quad (30)$$

Soil surface heat flux

The surface convection heat flux was incorporated to the model by imposing a heat flux at the top side as a boundary condition as follows [37]:

$$\left[-k \frac{\partial T_{surf}}{\partial z}\right]_{z=0} = CE - LR + SR - LE \quad (31)$$

where CE is the convective energy, LR is the long wave radiation emitted from the ground surface, SR is the absorbed solar radiations and LE is the latent heat due to evaporation. CE and LE are given by Mihalakakou et al. [37], LR and SR are given by Thiers and Peuportier [41].

The convective heat flux is given by:

$$CE = HTC_{surf} \cdot (T_{air} - T_{surf}) \quad (32)$$

where

$$HTC_{surf} = 0.5 + 1.2 \cdot u^{0.5} \quad (33)$$

The long wave radiation emitted from the ground is:

$$LR = \varepsilon_S \cdot \sigma \cdot \left(T_{surf}^4 - T_{air}^4\right) \quad (34)$$

Note that for LR the temperatures are in Kelvin (K).

The absorbed solar radiation is defined as:

$$SR = (1 - alb) \cdot G \quad (35)$$

The latent heat due to the evaporation is estimated by:

$$LE = 0.0168 \cdot f \cdot HTC_{surf} \cdot \left[103 \cdot T_{surf} + b_{lat} - \varphi \cdot (103 \cdot T_{air} + 609)\right] \quad (36)$$

f it is estimated as follows:

- For bare soils:
  - saturated soil: f = 1
  - moist soil: f = 0.6–0.8
  - dry soil: f = 0.4–0.5
  - arid soil: f = 0.1–0.2
- For grass covered soils the previous values are multiplied by 0.7

Analytical model "FLS"

The model of Zeng et al. [6] establishes the transient response at any point in the ground for the radial and the axial coordinates subject to a constant line heat source (FLS) in the rod. They formulated the temperature profile in the soil around the rod using the following formula:

$$\theta = \frac{q}{4\pi k_S} \int_0^L \left[\frac{\operatorname{erfc}\left(\frac{\sqrt{r^2+(z-h)^2}}{2\sqrt{\alpha t}}\right)}{\sqrt{r^2+(z-h)^2}} - \frac{\operatorname{erfc}\left(\frac{\sqrt{r^2+(z+h)^2}}{2\sqrt{\alpha t}}\right)}{\sqrt{r^2+(z+h)^2}} \right] dh \quad (37)$$

where

Table 2 – Soil parameters.

K_S [W/K m]	Conductivity	3.15
C_S [J/K m^3]	Heat capacity	2,240,000

$$\theta = T - T_0 \quad (38)$$

Results and discussion

The parameters of the system components (pipes and fluid) and the soil parameters used in the present simulation are given in Table 1 and Table 2.

Fig. 4 represents the impact of axial effects and the way of their consideration on the temperature distribution in the surrounding ground, a certain discrepancy of 0.606 °C between FVM and FLS models was observed and decreases with the increase of the radius. The ability of the analytical solution to treat these effects is limited by considering only the initial distribution of the undisturbed ground temperature which means the soil surface temperature remains constant and equal to the initial temperature over the operation period calculations. While the numerical solution has the ability to consider a time dependant surface temperature and this yields a remarkable difference of the distribution at almost the first 10 m.

In fact, when the heat pump is operating, the temperature distribution is not equal to the undisturbed ground temperature from the surface to the bottom, meaning, the cross-sections are not isotherms anymore, therefore instead of considering an imposed undisturbed temperature at the surface it would be more accurate if we consider an imposed heat flux as a boundary condition, which is the resultant of solar radiation that is uniform over the borehole surroundings at the surface and convection heat flux that has a non-uniform radial distribution this variation is due to the fact of the non-uniform radial temperature distribution in the vicinity of borehole induced by the operation of the heat pump. To introduce it to the model, we predict the undisturbed ground surface temperature numerically over the operation period (500 h) by treating the surface heat flux detailed in Ref. [37], then we compare it to the analytical prediction [39] as shown in Fig. 5; this helps to better account for seasonal effects, where the solar radiation, the ambient air temperature and velocity values are given for each hour over a year.

Once the undisturbed ground surface temperature is checked, we focus on the prediction of the surroundings temperature distribution for an operating heat pump. The vertical temperature distribution at the borehole vicinity over

Table 1 – Parameters of the system components (pipes and fluid).

Water parameters			Pipes parameters		
ρ [kg/m^3]	Density	999	r_{out} (mm)	Outer radius of outer pipe	115
μ_{wat} [kg/m s]	Viscosity	0.001138	e_{out} (mm)	outer pipe thickness	4
k_{wat} [W/K m]	Conductivity	0.59	r_{in} (mm)	Outer radius of inner pipe	40
C_{wat} [J/kg m^3]	Heat capacity	4,190,000	e_{in} (mm)	Thickness of inner pipe	2.4
W_{wat} [m^3/s]	Flow rate	5.8 10E-4	k_p (W/K m)	Pipes conductivity	0.4
T_{in} [°C]	Inlet temperature	1	L (m)	well depth	100

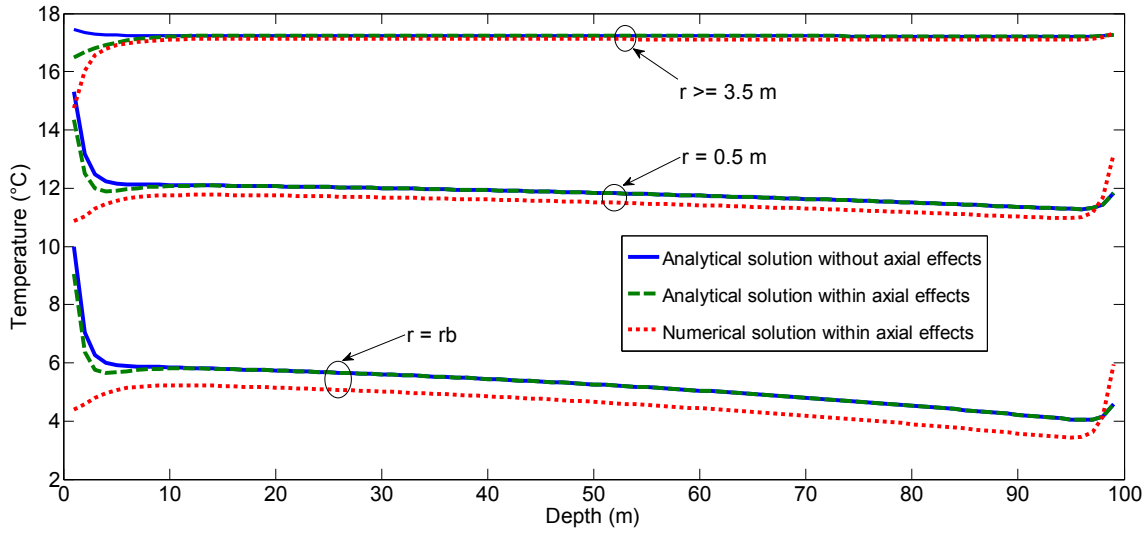

Fig. 4 – Different ways of considering axial effects.

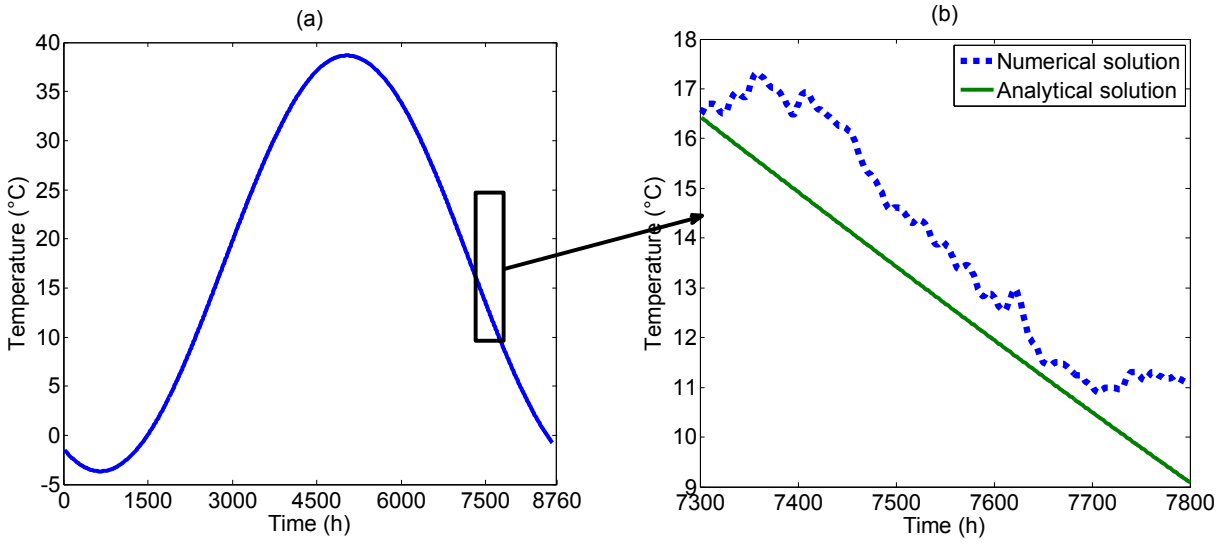

Fig. 5 – (a) The surface undisturbed temperature distribution using analytical prediction over a year; (b) Analytical and numerical predictions of the surface undisturbed temperature over the operating period.

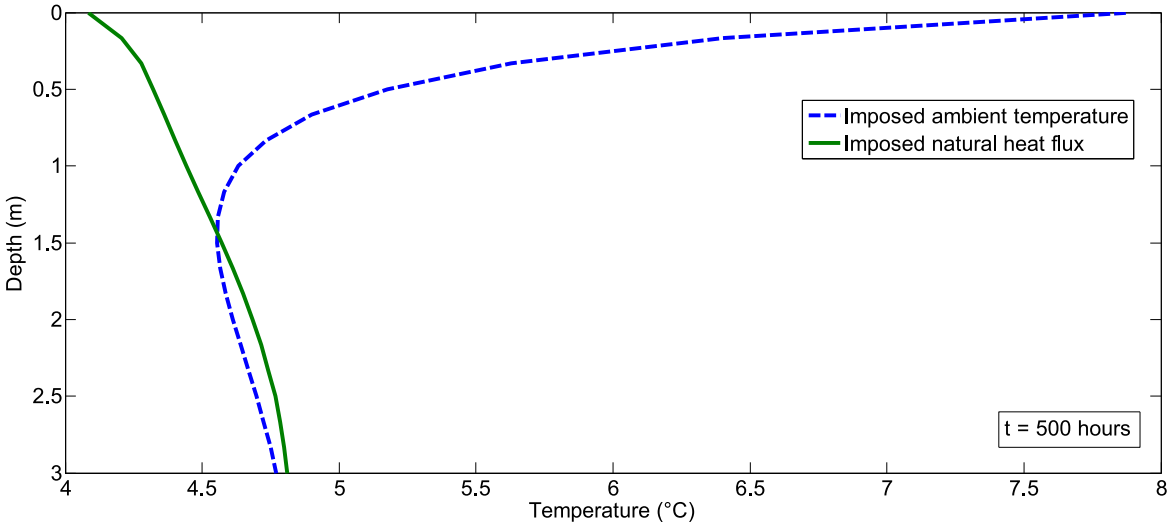

Fig. 6 – Comparison between axial effects treated by a variable surface temperature and a variable heat flux at the surface.

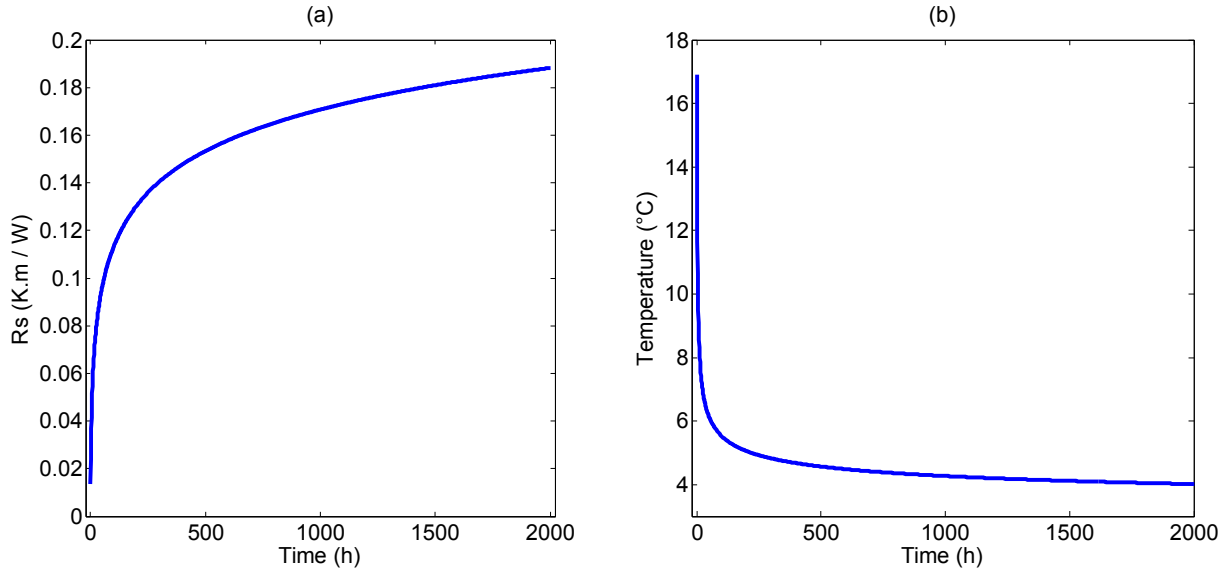

Fig. 7 – (a) The soil thermal resistance variation with the time; (b) the outlet fluid temperature over the operation period.

the first 3 m is shown in Fig. 5. The difference between the two approaches (imposed natural heat flux and imposed ambient temperature) was significant as shown in Fig. 5 and it affected soil temperature up to 1.4 m from the surface. This effect is expected to be greater for longer operation of heat pump.

Till now, it has been concluded (based on Figs. 4 and 6) that axial effects are more relevant for long operation period and shorter ground heat exchangers, and the effect of the dynamic heat flux along the depth would be more considerable for longer borehole heat exchangers. Fluid temperature prediction model of Beier et al. [36] was coupled to the ground numerical model. First the soil resistance of this model has been considered constant for the simulation period of 500 h and equals to the mean distribution in the present study and consequently the fluid temperature distribution remains constant. In fact this resistance is a time dependent value according to Carslaw and Jaeger [40] and it is shown in Fig. 7(a). The fluid temperature and heat rate distributions predictions are time dependent as well as the outlet temperature, thus the same thing for the outlet temperature shown in Fig. 7(b). Total heat input rate over time was predicted for a 2000 h of operation and it is given in Fig. 8.

The mean vertical fluid and heat flux distribution predictions in Fig. 9 refer to the features of instant distributions at each time step. It is remarkable that outlet temperature and withdrawn energy decrease overtime which could not satisfy the heat demand of the building, so in order to increase these values it is recommended to charge the soil thermally and/or couple the system with an energy storage system.

Time dependent fluid temperature distribution and the consideration of the physical phenomena which are the initial ground temperature distribution, a time dependent far field

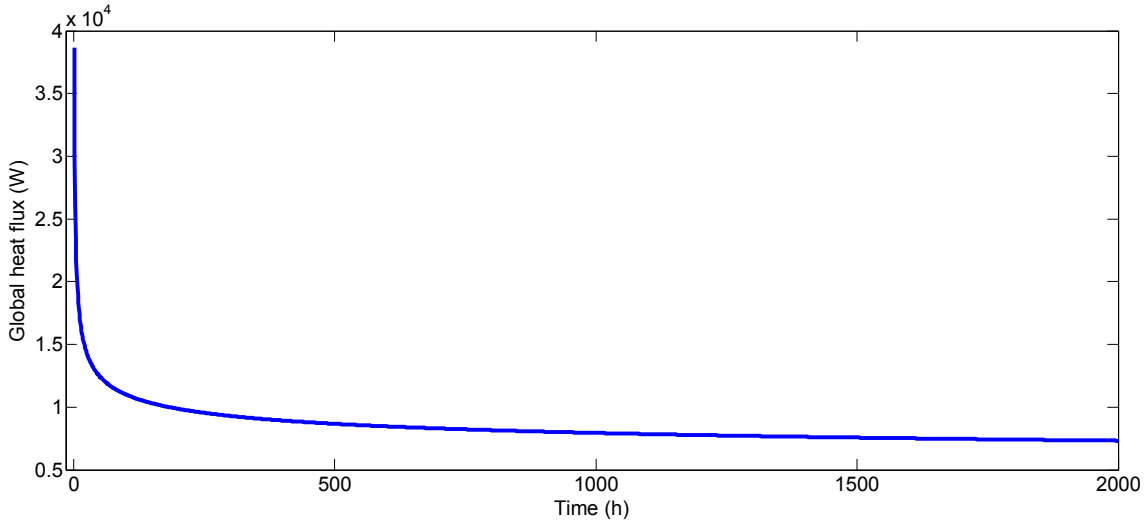

Fig. 8 – Total exchanged heat as a function of time.

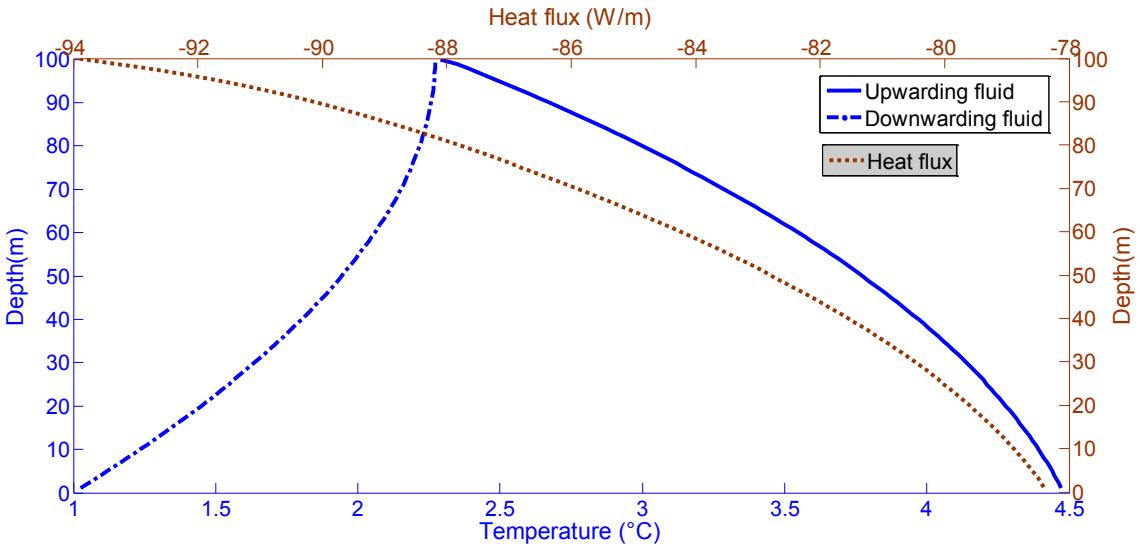

Fig. 9 – The mean vertical distributions of the fluid temperature and the exchanged heat rate.

temperature distribution, a surface heat flux rather than the undisturbed ground surface temperature in the soil region lead to a closer to the reality thermal analysis in the soil, so a long term simulation is shown in Fig. 10.

Time series of fluid temperature at different depths (at the surface z = 0 m, at the middle of the BHE z = 50 m and at the BHE bottom z = 100 m) during 2000 h of operation is given in Fig. 10(a). For the three depths the temperature decreases with time. Comparing the three historical it is remarkable that the bottom historical has the lowest values which mean that the heat exchange rate is at its maximum at the bottom of the BHE.

Radial temperature distribution at depth of 50 m and after 2000 h of operation is given in Fig. 10(b). It can be seen that the temperature increased with increasing distance from the heat exchanger. In other words, the coldest regions are the closest ones to the BHE wall.

Temperatures along depth are given in Fig. 10(c). As can be seen, the coldest distributions are the closest ones to the BHE, also, for the far field radius (9 m), where the temperature profile is the undisturbed ground temperature profile which becomes constant since almost a depth of 15 m, but it is not the case for closer distances to the BHE, the temperature doesn't become constant any more, it is always variable with depth, this is due to the effect of the dynamic behaviour of the BHE which is shown in Fig. 9.

The second step is to predict the thermal interaction between neighbouring boreholes. The thermal interactions occur when more than a heat source or sink affect the same point, meaning: two or more heat sources or sinks start

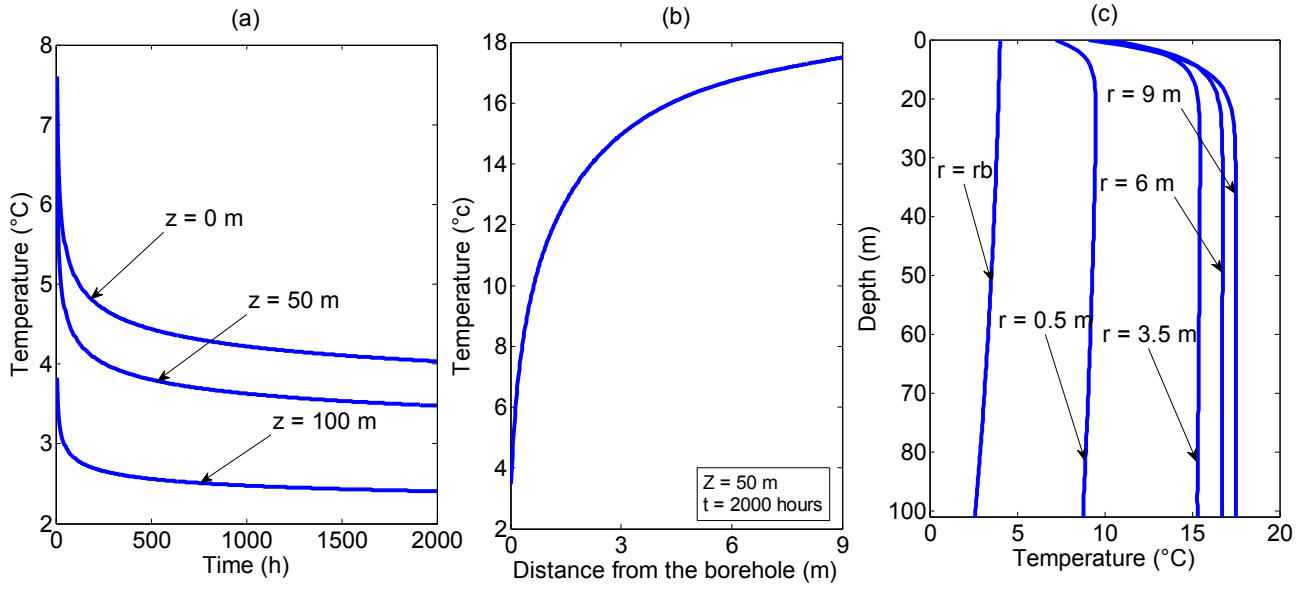

Fig. 10 – (a) Historical of different points at the borehole vicinity; (b) Radial temperature distribution; (c) Vertical distributions at several radius values.

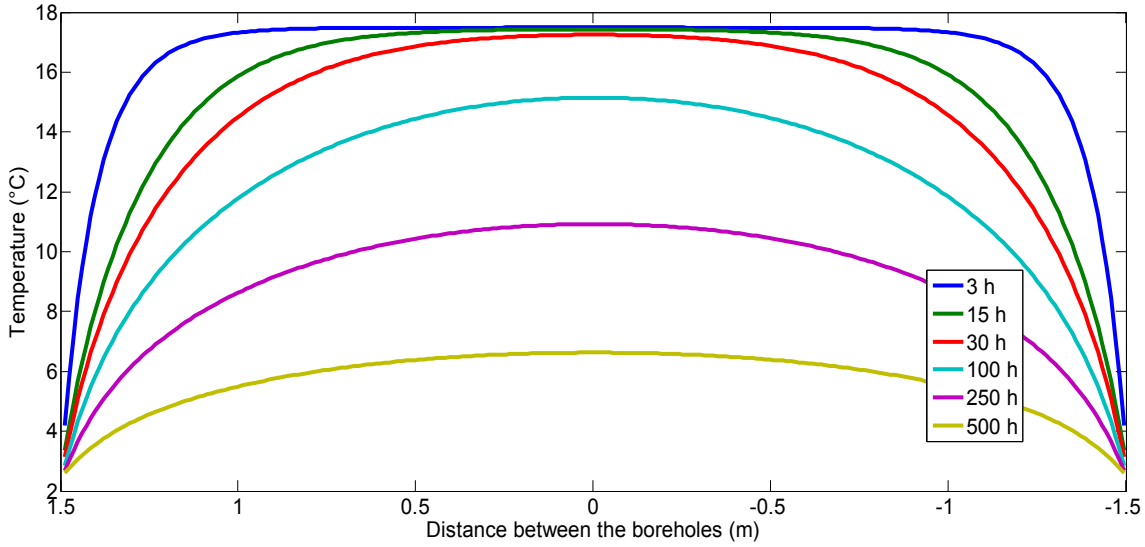

Fig. 11 – The historical of the interferences at the bottom of the borehole.

interacting when they become withdrawing or injecting heat to the same point. In other words, interactions start when the fronts of two or more heat waves just meet each others and disturb the temperature of this meeting point together.

The borehole spacing is a function of BHE heat input rate, the soil thermal diffusivity and climate region; it varies from system to another in a way to keep performances as high as possible. For example, Baser et al. [42] used a borehole spacing of 2.5 m, Bandos et al. [8] used an inter-borehole distance of 3 m, and Marcotte et al. [9] used a borehole spacing of 3.33 m. In the present study a borehole spacing of 3 m was chosen, which is a common value for the analysis of GSHP systems. The thermal interferences evolution with time at the bottom of the borehole is shown in Fig. 11 where the phenomena (interferences) are amplified. Borehole wall temperatures vary with time this is due to the time dependent fluid temperature inside the boreholes.

From Fig. 12 we can get the time of beginning of the interferences function of the depth, this time corresponds to the decrease of 0.8 °C than the undisturbed temperature at the midway between the boreholes. Thermal interference starts at the bottom of the borehole where the amount of the exchanged heat is higher and this is relating to Fig. 8, this is for the case when the fluid enters the inner pipe, for the one when the fluid enters the annulus, the exchanged heat rate decrease from the top to the bottom which leads to higher interactions at the top side where there are temperature fluctuations. When the borehole diameter is greater more energy can be withdrawn. In addition soil having higher thermal conductivity contributes to the higher heat extraction rate. These parameters have an effect on the thermal interference.

Figs. 13 and 14 represent the temperature distribution in the ground at the bottom in a surface plot, where the isotherms projection on the (XY) plan represents the contour of

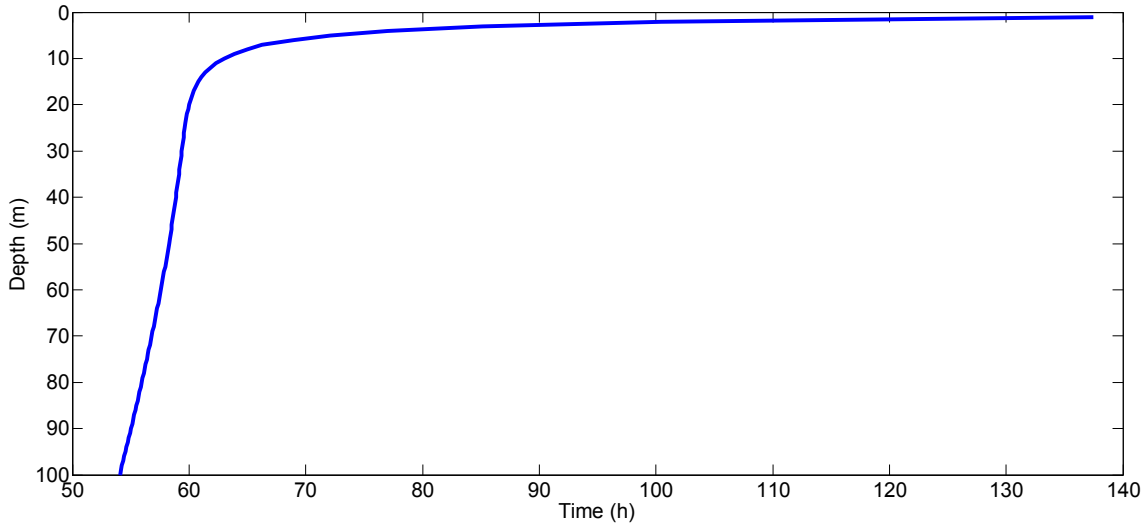

Fig. 12 – Distribution of the time of beginning of thermal interferences along the depth.

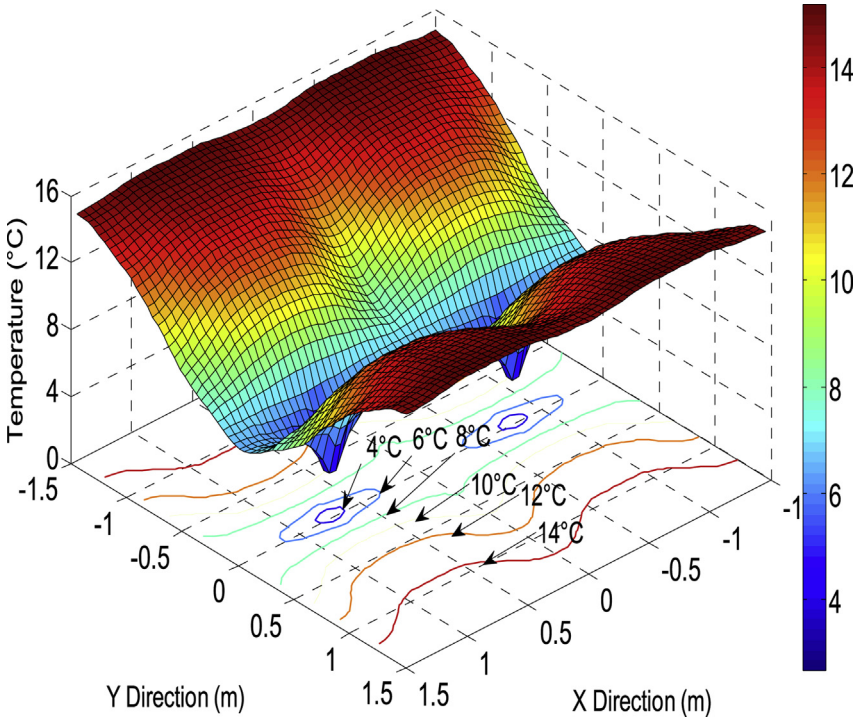

Fig. 13 – Cross section temperature distributions at the bottom of the borehole after 500 h of operation.

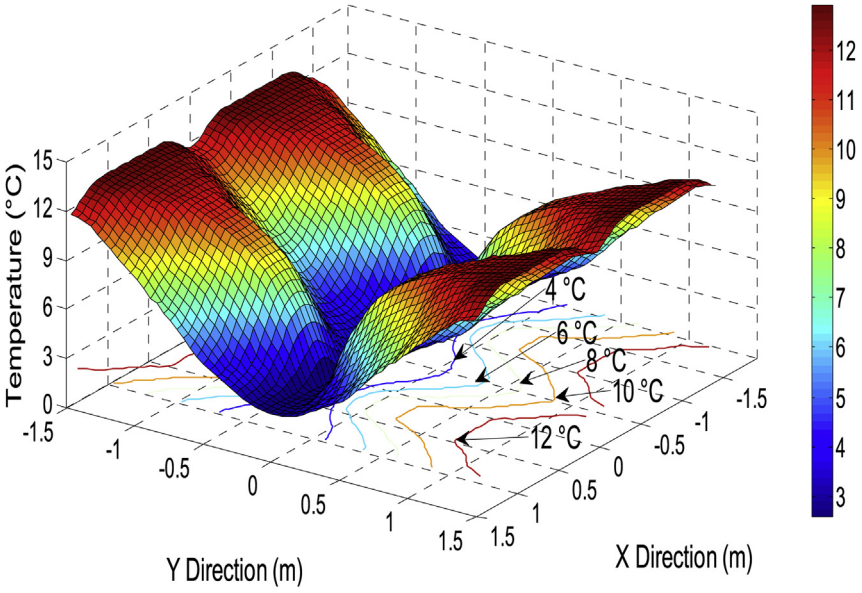

Fig. 14 – Cross section temperature distributions at the bottom of the borehole after 1000 h of operation.

that cross section. As seen in Fig. 13, hot regions are closer to the boreholes' vicinity than it in Fig. 14, in other word the cold in Fig. 14 is occupying a bigger surface which means the cold is invading the surrounding soil and so interferences are emphasized with the increase of time.

Conclusion

In the present paper thermal interferences are investigated under seasonal effects and a dynamic exchanged heat flux for a vertical coaxial borehole heat exchanger (BHE). Seasonal effects have been treated doing a physical balance between convective heat transfer between the ambient air and the soil surface and solar radiations.

First, axial and seasonal effects have been studied separately by building a transient 2D FVM model then coupling it to a fluid model to introduce the dynamic behaviour of the heat flux. In addition, a source term has been added to the top boundary of the domain in order to introduce the convective heat exchange and solar radiations. It has been concluded that axial and seasonal effects, under the new surface heat balance

(convection and solar radiation), are only relevant for short borehole depths and for long operation periods, and the dynamic heat flux along the depth is more considerable for long boreholes depths. This allows us to obtain a more real physical situation, which means a more accurate temperature profiles in the surrounding ground can be predicted, this advocates the better way to study thermal interferences in a borehole field.

Then, the 2D model has been extended to a quasi 3D model. This part of the study allows us to predict the start time of thermal interferences for a given heat load demand and borehole spacing in order to avoid them by giving a greater value of the separation distance compatible to the required heat load and the period of operation. This allows us to extract the greatest amount of energy using a less occupied surface, allowing optimization of the separation distance. To clarify, avoiding these phenomena avoids the extreme local cooling to guarantee a given seasonally variable energy demand, meaning, the fluid temperature is higher, so the performance of the heat pump is higher.

The results from this study show that the soil resistance is increasing with time, consequently the outlet temperature is decreasing with time, and this causes the decrease of the performance of the heat pump, for this reason it is recommend to couple the system with a solar thermal soil recharging system and/or couple the system with an energy storage system.

REFERENCES

[1] Yuksel YE, Ozturk M. Thermodynamic and thermoeconomic analyses of a geothermal energy based, integrated system for hydrogen production. Int J Hydrogen Energy 2017;42:2530–46.

[2] Ramazankhani ME, Mostafaeipour A, Hosseininasab H, Fakhrzad MB. Feasibility of geothermal power assisted hydrogen production in Iran. Int J Hydrogen Energy 2016;41:18351–69.

[3] Belatreche D, Bentouba S, Bourouis M. Numerical analysis of earth air heat exchangers at operating conditions in arid climates. Int J Hydrogen Energy 2017;42:8898–904.

[4] Antonov S, Helsen L. Robustness analysis of a hybrid ground coupled heat pump system with model predictive controls. J Process Control 2016;47:191–200.

[5] Bendaikha W, Larbi S, Bouziane M. Feasibility study of hybrid fuel cell and geothermal heat pump used for air conditioning in Algeria. Int. J Hydrogen Energy 2011;6:4253–61.

[6] Zeng HY, Diao NR, Fang ZH. A finite line-source model for boreholes in geothermal heat exchangers. Heat Transfer Asian Res 2002;31:558–67.

[7] Lamarche L, Beauchamp B. A new contribution to the finite line-source model for geothermal boreholes. Energy Build 2007;39:188–98.

[8] Bandos TV, Montero A, Fernández E, Santander JLG, Isidro JM, Pérez J, et al. Finite line-source model for borehole heat exchangers: effect of vertical temperature variations. Geothermics 2009;38:263–70.

[9] Marcotte D, Pasquier P, Sheriff F, Bernier M. The importance of axial effects for borehole design of geothermal heat-pump systems. Renew Energy 2010;35:763–70.

[10] Molina-Giraldo N, Blum P, Zhu K, Bayer P, Fang Z. A moving finite line source model to simulate borehole heat exchangers with groundwater advection. Int J Therm Sci 2011;50:2506–13.

[11] Kurevija T, Vulin D, Krapec V. Effect of borehole array geometry and thermal interferences on geothermal heat pump system. Energy Convers Manag 2012;60:134–42.

[12] Hecht-Méndez J, De Paly M, Beck M, Bayer P. Optimization of energy extraction for vertical closed-loop geothermal systems considering groundwater flow. Energy Convers Manag 2013;66:1–10.

[13] Li M, Lai ACK. Analytical model for short-time responses of ground heat exchangers with U-shaped tubes: model development and validation. Appl Energy 2013;104:510–6.

[14] Wagner V, Blum P, Kübert M, Bayer P. Analytical approach to groundwater-influenced thermal response tests of grouted borehole heat exchangers. Geothermics 2013;46:22–31.

[15] Cimmino M, Bernier M, Adams F. A contribution towards the determination of g-functions using the finite line source. Appl Therm Eng 2013;51:401–12.

[16] Li Y, Mao J, Geng S, Han X, Zhang H. Evaluation of thermal short-circuiting and influence on thermal response test for borehole heat exchanger. Geothermics 2014;50:136–47.

[17] Zhang C, Chen P, Liu Y, Sun Peng D. An improved evaluation method for thermal performance of borehole heat exchanger. Renew Energy 2015;77:142–51.

[18] Choi W, Ooka R. Effect of natural convection on thermal response test conducted in saturated porous formation: comparison of gravel-backfilled and cement-grouted borehole heat exchangers. Renew Energy 2016;96:891–903.

[19] Yavuzturk C, Spitler JD, Rees SJ. A transient two-dimensional finite volume model for the simulation of vertical U-tube ground heat exchangers. ASHRAE Trans 1999;105(2):465–74.

[20] Asinari P. Finite-volume and finite-element hybrid technique for the calculation of complex heat exchangers by semiexplicit method for wall temperature linked equations (SEWTLE). Torino, Italy. 2004. http://porto.polito.it/1405818/1/preprint_Asinari_NHTB_2004a.pdf [Accessed 13 November 2016].

[21] Kim EJ, Roux JJ, Rusaouen G, Kuznik F. Numerical modelling of geothermal vertical heat exchangers for the short time analysis using the state model size reduction technique. Appl Therm Eng 2009;30:706–14.

[22] Wołoszyn J, Goła A. Modelling of a borehole heat exchanger using a finite element with multiple degrees of freedom. Geothermics 2013;47:13–26.

[23] Yoon S, Lee SR, Go GH. A numerical and experimental approach to the estimation of borehole thermal resistance in ground heat exchangers. Energy 2014;71:547–55.

[24] Koohi-Fayegh S, Rosen MA. Examination of thermal interaction of multiple vertical ground heat exchangers. Appl Energy 2014;97:962–9.

[25] Pasquier P, Marcotte D. Joint use of quasi-3D response model and spectral method to simulate borehole heat exchanger. Geothermics 2014;51:281–99.

[26] Luo J, Rohn J, Bayer Manfred, Priess Anna. Thermal performance and economic evaluation of double U-tube borehole heat exchanger with three different borehole diameters. Energy Build 2013;67:217–24.

[27] BniLam N, Al-Khoury R. A spectral model for heat transfer with friction heat gain in geothermal borehole heat exchangers. Appl Math Model 2016;40:7410–21.

[28] Hein P, Kolditz O, Görke UJ, Bucher A, Shao H. A numerical study on the sustainability and efficiency of borehole heat exchanger coupled ground source heat pump systems. Appl Therm Eng 2016;100:421–33.

[29] Hein P, Zhu K, Bucher A, Kolditz O, Pang Z, Shao H. Quantification of exploitable shallow geothermal energy by

using borehole heat exchanger coupled ground source heat pump systems. Convers Manag 2016;127:80–9.
[30] Baek SH, Yeo MS, Kim KW. Effects of the geothermal load on the ground temperature recovery in a ground heat exchanger. Convers Manag 2017;136:63–72.
[31] Gallero FJG, Maestre IR, Gomez PA, Blaquez JLF. Numerical and experimental validation of a new hybrid model for vertical ground heat exchangers. Energy Convers Manag 2015;105:511–8.
[32] Florides G, Theofanous E, Iosif-Stylianou I, Tassou S, Christodoulies P, Zomeni Z, et al. Modeling and assessment of the efficiency of horizontal and vertical ground heat exchangers. Energy 2013;58:655–63.
[33] Farouki OT. Thermal properties of soils. Hanover, New Hampshire, USA: United States Army Corps of Engineers Cold Regions Research and Engineering Laboratory; 1981.
[34] Patankar SV. Numerical heat transfer and fluid flow. New York, USA: McGraw Hill Book Company; 1980. ISBN: 0-07-0487405.
[35] Versteeg H K, Malalasekera, An introduction to computational fluid dynamics, the finite volume method.
[36] Beier RA, Acuña J, Mogensen P, Palm B. Borehole resistance and vertical temperature profiles in coaxial borehole heat exchangers. Appl Energy 2013;102:665–75.
[37] Mihalakakou G, Santamouris M, Lewis JO, Asimakopoulos DN. On the application of the energy balance equation to predict ground temperature profiles. Sol Energy 1997;60(3/4):181–90.
[38] Eskilson P. Thermal analysis of heat extraction boreholes. Doctoral Thesis. Lund, Sweden: Department of Mathematical Physics, University of Lund; 1987. www.buildingphysics.com/Eskilson1987.pdf [Accessed 13 November 2016].
[39] Ozgener O, Ozgener L, Tester JW. A practical approach to predict soil temperature variations for geothermal (ground) heat exchangers applications. Int J Heat Mass Transf 2013;62:473–80.
[40] Carslaw HS, Jaeger JC. Conduction of heat in solids. 2nd ed. Oxford: Oxford University Press; 1959.
[41] Thiers Stéphane, Peuportier Bruno. Modélisation thermique d'un échangeur air-sol pour le rafraichissement de bâtiment. Journée thématique SFT-IBPSA: froid solaire et confort d'été, April 2007, Aix-les-Bains, France. <HAL-00216068>. 2007. p. 96–103. https://hal.archives-ouvertes.fr/HAL-00216068/document [Accessed 18 February 2017].
[42] Başer T, Lu N, McCartney JS. Operational response of a soil-borehole thermal energy storage system. Am Soc Civ Eng 2015. http://dx.doi.org/10.1061/(ASCE)GT.1943-5606.0001432. https://www.pc-progress.com/Images/Personal/NLu/Publications/NLJ93201508.pdf [Accessed 18 February 2017].